Terr. Atmos. Ocean. Sci., Vol. 32, No. 6, Part II, 1107-1115, December 2021 doi: 10.3319/TAO.2021.12.15.03

Generic-level identification of Astriclypeidae based on incomplete onsite-specimens from Yehliu Geopark, Taiwan

Ammu Sankar Senan * and Robert Swisher

Department of Geosciences, National Taiwan University, Taipei City, Taiwan

Article history:

Received 14 June 2021
Revised 3 December 2021
Accepted 15 December 2021

Keywords:

Landmark analysis, Principal Component Analysis, Astriclypeidae, Lunule variability, Miocene

Citation:

Senan, A. S. and R. Swisher, 2021: Generic-level identification of Astriclypeidae based on incomplete onsite-specimens from Yehliu Geopark, Taiwan. Terr. Atmos. Ocean. Sci., 32, 1107-1115, doi: 10.3319/TAO.2021.12.15.03

ABSTRACT

Incompleteness in fossil specimens is the main obstacle that has to be overcome with the identification of fossils and the analyses using them. Landmark analysis is a tool that can be used to understand the variations in different organismal factors based on morphology with adequate preparation and properly aligned photographs of specimens. The goal is to apply these methods to assess generic level identification of Miocene Astriclypeidae, including *Astriclypeus* and *Echinodiscus*, based on incomplete onsite specimens from the Yehliu Geopark, Taiwan; a locality in where the removal of fossil specimens is not permitted. Two datasets were chosen utilizing the available fossil specimens from the site: a three-point dataset and a seven-point dataset. Linear measurements of onsite specimens were also recorded for comparison. Results from Principal Component Analysis (PCA) showed that samples of *Astriclypeus* and *Echinodiscus* formed distinct clusters based on three-point dataset. A similar trend with distinct clusters for the two genera was also evident with the seven-point dataset. Furthermore, the effectiveness of this method is reinforced by the results of the independent study using the traditional method with linear measurements. Geometric morphometrics can specifically identify where morphological variation occurs and is concentrated based on the chosen landmark arrays, and such morphological variations cannot be detected easily with the linear and angle measurements alone. This study shows that the landmark analysis can be used efficiently for a generic level identification based on incomplete specimens.

1. INTRODUCTION

Statistical shape analysis or geometric morphometrics is a structured approach to the analysis of landmarks for shape variation (Kendall 1984; Bookstein 1992). A geometric morphometric approach is bound up with the concept of the landmark. In the context of geometric morphometrics a landmark is defined as "a specific point on a biological form or image of a form located according to some rule" (Bookstein 1992). Geometric morphometric data consist of 2D or 3D Cartesian landmark coordinates (relative to some arbitrarily chosen origin and axes) (Bookstein et al. 1991; Webster and Sheets 2010; Schlüter 2016). When we use the 2D landmark coordinate locations, the coordinate point locations are referenced to linear distances along independent *x* and *y* axes they record the position of each landmark relative to every other landmark precisely. Different landmark configurations may be needed for different studies, as when some subset of the total sample is missing particular landmarks.

Echinoids are divided into two distinct categories; Regularia and Irregularia (paraphyletic classification) sea urchins. Regular urchins have an almost spherical symmetry, while irregular urchins display varying degrees of bilateral symmetry (Chao 2000). Irregular urchins with flattened tests and key-hole shaped perforations (lunules) toward the rear of the endoskeleton are commonly known as sand dollars or keyhole urchins and belong to the order Clypeasteroida; members of this order have developed near radial symmetry (Swisher and Lin 2019) includes 150 extant species and 750 fossil species (Mooi 1989) and are first known from the late Paleocene (Kier 1982; Smith 1984, 2001; Kroh and Smith 2010; Mihaljević et al. 2011; Mancosu and Nebelsick 2017). The characteristics of sand dollars such as flat test,

* *Corresponding author*
E-mail: ammusankars93@gmail.com

spine differentiation, food grooves and lunules are related to a particular combination of burrowing and probably sieve feeding in sandy sediments (Seilacher 1979).

Irregular sea urchins are common benthic macro-organisms along the coasts of Taiwan (Chao 2000); despite this there have only been a few papers published studying the systematic collections or descriptions of irregular urchins in Taiwan (Ohshima 1927; Hayasaka 1947; Peng and Tiao 1971; Shigei 1981; Wang 1982, 1983, 1984; Chao 2000). Fossil irregular echinoids of the Genera *Echinodiscus* with two lunules (Wang 1982) and *Astriclypeus* with five lunules (Nisiyama 1935) are found abundant in the Taliao Formation of Yehliu from Yehliu Geopark, Taiwan. However, the specimens present in this setting are incomplete and highly fragmented, which restricts accurately distinguishing the lunule numbers, making identification of the different genera problematic. This study implements a landmark based image analysis of the incomplete specimens for the generic identification of Astriclypeidae present in the Geopark, Taiwan. This is a case study to determine methodologies for generic level identification of incomplete clypeasteroids specimens within a population, potentially forming a foundation for broader population studies in more likely settings.

2. METHODOLOGY

A total of 55 specimens, which includes 18 specimens of *Astriclypeus* and 37 specimens of *Echinodiscus*, were examined. The specimens were observed thoroughly and identified into two different genera prior to the analysis. These specimens are from the early Miocene Taliao Formation from the Yehliu Geopark (25°12'21.6"N, 121°41'30.5"E) (Fig. 1a). Since all specimens were photographed directly from the site for the geometric morphometrics analysis, extreme care was taken to standardize specimen images and minimalize errors during specimen photography, avoiding tilting of the specimen (Fig. 1b). Specimen images were oriented parallel to the bilateral plane of symmetry and the periproct has been positioned posteriorly. Adobe Photoshop (Adobe Systems Incorporated 2002) software was used to adjust the orientations of the photographs to accurate positions. Specimens with the aboral surface exposed were more numerous compared to the oral surface in the field. Therefore, only specimens with exposed aboral surfaces were analyzed in this study. Digitization of landmark data for specimens was done using the software TpsDig 2.31 (Rohlf 2015, 2018). Three landmark points were considered from the aboral surface, one from the midpoint of the apical disc and the other two from the maximum protruding point on both curving sides of the posterior lunules (Figs. 2a, b). This is the least number or landmarks that can generate a calculable area and represents the minimal data needed to assess generic level differentiation within the data set. Importantly, particularly when using fragmentary data sets as fossil data sets commonly are, this landmark configuration provides a means to quantitatively distinguish between the study samples used in this analysis when only this small section of the test is available for analysis. Potentially, this can expand the number of specimen able to be added to and examined in a data set. This methodology could be applied towards fragmentary population samples and ecological studies of the examined groups, and potentially towards the analysis of other Clypeasteroids. A three-point landmark analysis, such as this, could also be applied to other lunule bearing sections of Clypeasteroids as a means to minimally quantify and distinguish between fragmentary data sets. All 55 specimens analysed had either of the posterior lunules and the apical disc preserved and hence used for the three landmark point analysis. Only 21 of the specimens had both the lunules and the central apical disc preserved within the data set; these have been utilized for the seven landmark data analysis. Posterior left lunules, when considering the aboral surface, were preserved more often when compared to the posterior right lunules. Therefore, the posterior left lunules and the midpoint of the apical disc were considered for the landmark digitization, while specimens with posterior right lunules were digitally mirrored to the left for analyses and to increase sample size of the data set. The seven landmark points were digitized from more complete specimens that have both the posterior lunules and the centre of the apical disc preserved. Again, only specimens with exposed aboral surfaces were considered for these measurements (Figs. 2c, d). Of the seven landmarks used, the first five points are consistent with the landmarks used in the three-point analysis; one from the midpoint of the apical disc on the aboral surface and the other four from the maximum protruding point on both curving sides of the posterior left and right lunules. The extra two landmarks are taken from the midpoint of the length from the line joining the upper most protruding points of the left and right lunules and the lower most protruding points of the left and right lunules at the intersection with the midline suture (Figs. 2c, d).

In addition, onsite measurements were taken for obtaining the length and width of the lunules (Fig. 3) with the Vernier Caliper (0.01 mm precision). The length and width are measured in mm and is used for calculating the area as well as the length to width ratio for the purpose of traditional morphometric analysis. Geometric morphometric methodology for this analysis followed the outline given by Bookstein (1992) and Webster and Sheets (2010). Morphological terminologies followed the usages in Mooi (1989).

MORPHOJ 1.07a (Klingenberg 2011) software was used for the statistical analysis. This software provides a flexible and user-friendly platform for a broad range of morphometric analyses for two- or three-dimensional landmark data (Klingenberg 2011). Digitized landmark data were imported to the software for analysis where the shape information was extracted from the data with a Procrustes

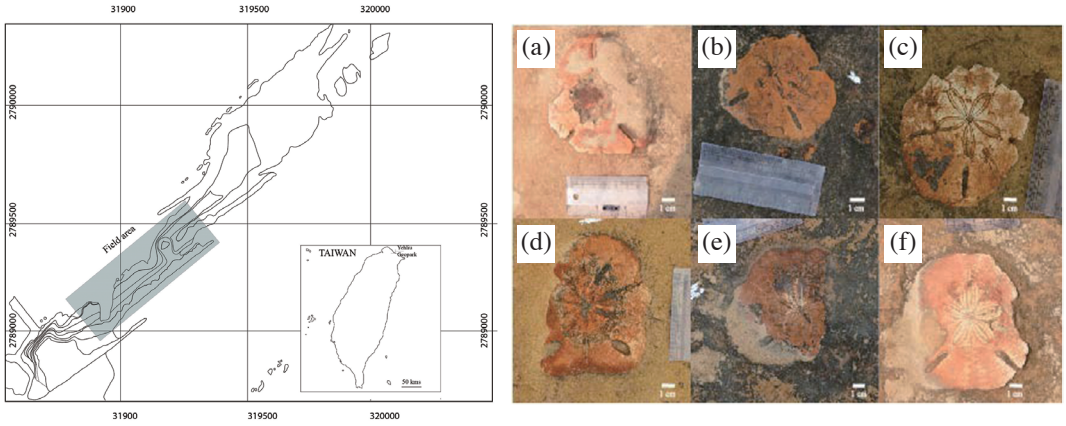

Fig. 1. (a) Map of studied areas at the Yeliu Geopark, Taiwan. (b) Examples for onsite specimens photographed for the study. (a), (b), and (c) are *Astriclypeus*; (d), (e), and (f) are *Echinodiscus* specimens.

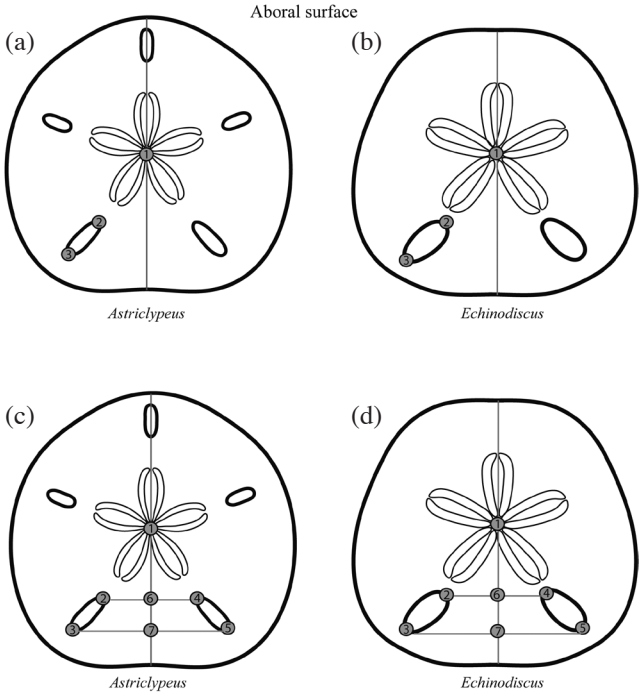

Fig. 2. Landmark configuration for the geometric morphometric analysis. Landmarks are specified as numbers inside the circle. (a) and (c) landmark points for *Astriclypeus* marked in the aboral surface. (b) and (d) landmark points for *Echinodiscus* marked in the aboral surface. Line showing the bilateral plane of symmetry is passing through the center of the apical plate where landmark point (1) is located. Landmark points (2) and (4) are the outermost protruding point on the curved side of lunule towards the apical plate. Landmark points (3) and (4) are the outermost point protruding on the curved side of lunule towards the boundary. Landmark point (6) is at the point where the bilateral plane of symmetry coincides with the plate boundary and the midpoint of the landmarks (2) and (4). Landmark point (7) is at the point where the bilateral plane of symmetry coincides with the plate boundary and the midpoint of the landmarks (3) and (7).

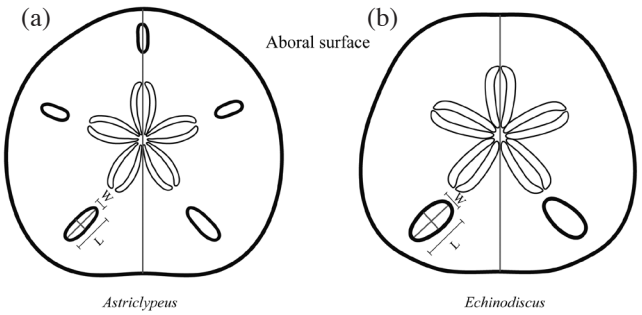

Fig. 3. Traditional morphometric analysis. Length (L) and width (W) of the lunules measured. Line showing the bilateral plane of symmetry is passing through the center of the apical plate.

superimposition (Dryden and Mardia 1998). MORPHOJ implements a full Procrustes fit and projection onto the tangent. A Procrustes analysis (Rohlf and Slice 1990) is used to superimpose the specimens to a common coordinate system in accordance to the variation in their position, size and orientation. From these Procrustes aligned coordinates, a set of shape variables can be obtained (Bookstein 1992), which in turn will be used in the multivariate statistical analyses. It is important that prior to any analysis a Procrustes fit is performed as the shape of each specimen is rescaled to unit centroid size, which removes the information on size. The centroid size data was obtained then converted to log centroid size in MORPHOJ and used for an F-test of comparison of variance between the two datasets in Past statistical software (Hammer et al. 2001). Analysis of Variance (ANOVA) was conducted of using the mean centroid values and regression scores obtain and processed through MorphoJ; this analysis was used to understand if the variance between the means of the two populations were significantly different and Regression analysis for understanding the variation. Principal Component Analysis (PCA) was performed on the Procrustes fit data set. PCA is a statistical technique for reducing the number of variables when a significant correlation between the variables is present (Monteiro 2013). PCA can be used to examine the main features of shape variation in a sample and as an ordination analysis for examining the arrangement of specimens in morphospace (Klingenberg 2011).

3. RESULTS

3.1 Geometric Morphometric Data Analysis

Generic level identification for the specimens was conducted using Principal Component Analysis (PCA). The PCA values obtained from the three landmark point data set and the seven landmark point data set for the aboral surface are summarized (Table 1). PCA 1 and 2 constitute a cumulative sum of 100% for the three landmark point data set, while PCA 1, 2, 3, and 4 make up for a cumulative sum of 94.68% for the seven landmark point data set. Two distinct clusters can be observed, distinguishing and separating the two genera *Astriclypeus* and *Echinodiscus*, in both the three landmark point and seven landmark point data sets (Figs. 4a - d). PCA 1 vs. PCA 2 (Fig. 4a) shows variation and clustering of the *Astriclypeus* and *Echinodiscus* for the three landmark point PCA plot while PCA 1 vs. PCA 2 indicates distinctive clusters of the two genera for the seven landmark point PCA plot (Fig. 4b). The two plots, PCA 1 vs. PCA 3 (Fig. 4c) and PCA 1 vs. PCA 4 (Fig. 4d) show clustering of the two genera similar to the previous seven landmark point PCA plot of PCA 1 vs. PCA 2.

3.2 Traditional Morphometric Data Analysis

Two plots are presented here based on the linear measurements of lunules (Figs. 5a, b). The first one is Area (L*W) vs. Length (L) and the second one is Area (W*L) vs. Ratio (W/L). Both plots show distinct clusters for studied samples of *Astriclypeus* and *Echinodiscus*. Although lunule length (L) and ratio (W/L) are overlapping for *Astriclypeus* and *Echinodiscus* samples, lunule area (W*L) is the key factor that separates the two clusters in both plots.

3.3 Univariate Analysis (F-Test)

An F-test was conducted for both the three landmark point data and the seven landmark point data in PAST3 software to understand whether the means of the clusters are statistically different with the log centroid size. The P values for both the three landmark point data and the seven landmark point data obtained was less than 0.05, hence significant and therefore rejects the null hypothesis being tested were there is no difference between the means of the clusters in both the cases.

3.4 Analysis of Variance (ANOVA)

The regression analysis was done by MORPHOJ software. The results for the 3 landmark point data and the seven landmark point data shows distinctive clustering (Figs. 6a, b) for the analysis. For the 3 landmark point analysis data was

Table 1. PCA results for the 3-points dataset and the 7-points dataset.

Principal Axis	PCA 1	PCA 2	PCA 3	PCA 4	Sum
3-points landmark analysis	62.22%	37.77%	--	--	100%
7-points landmark analysis	66.73%	13.68%	9.73%	4.53%	94.68%

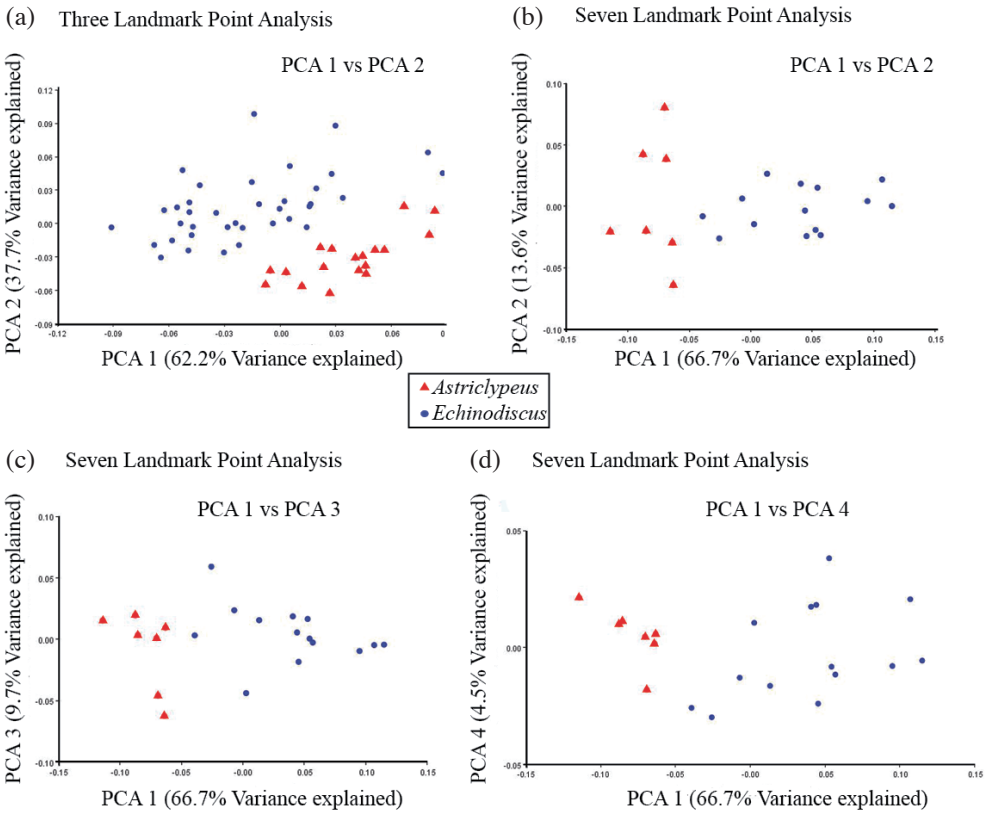

Fig. 4. Principal Component Analysis (PCA) plots for the landmark data for the both genera: *Astriclypeus* and *Echinodiscus*. (a) PCA plot for the three landmark point data. PCA 1 is represented in the x-axis and PCA 2 in the y-axis. PCA 1 and PCA 2 is accounted for 100% of morphological variance, where PCA 1 shows 62.2% variance and PCA 2 shows 37.7% Variance. (b) PCA for seven landmark point data. PCA 1 is represented in the x-axis and PCA 2 in the y-axis. PCA 1 and PCA 2 are accounted for 80.3% variance. PCA 1 explains 66.7% of the total variance and PCA 2 explains 13.6%. (c) PCA plot for the seven landmark point data. PCA 1 is represented in the x-axis and PCA 3 in the y-axis. PCA 1 and PCA 2 are accounted for 76.4% variance. PCA 1 explains 66.7% of the total variance and PCA 3 explains 9.7%. (d) PCA plot for the seven landmark point data. PCA 1 is represented in the x-axis and PCA 4 in the y-axis. PCA 1 and PCA 4 are accounted for 71.2% variance. PCA 1 explains 66.7% of the total variance and PCA 4 explains 4.5%.

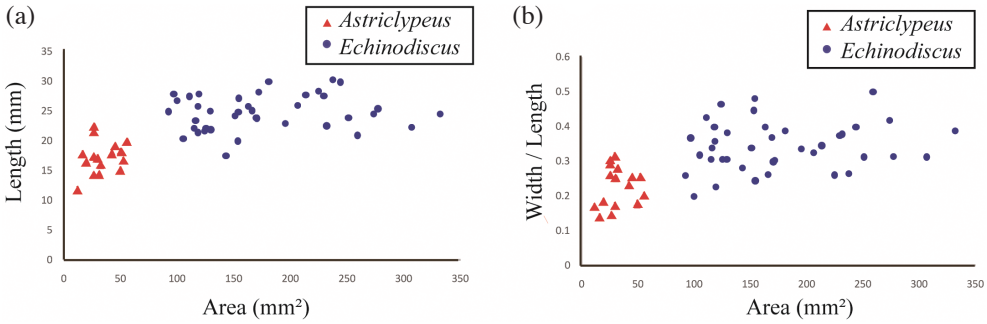

Fig. 5. Bivariate plots from the traditional morphometric analysis method using the length and width data for the lunules are shown here for the both genera: *Astriclypeus* and *Echinodiscus*. (a) Plot for area (mm^2) vs. length (mm) of the lunule. Area (L*W), which is the multiplied value of the length and width are represented in the x-axis and length (mm) in the y-axis. (b) Plot for area (mm^2) vs. width (mm) divided length (mm), (W/L) of the lunule. Area (L*W), which is the multiplied value of the length and width are represented in the x-axis and the ratio of width (mm) to length (mm), (W/L) is in the y-axis.

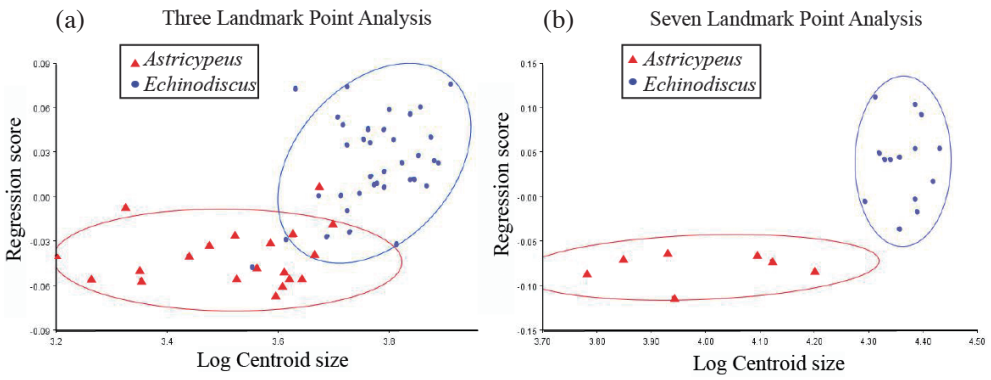

Fig. 6. Regression analysis results for three landmark point data and seven landmark point data are shown here. (a) Plot for Log centroid size vs. regression score for the three landmark point analysis. (b) Plot for Log centroid size vs. regression score for the seven landmark point analysis.

taken from 55 specimens. The value of total sum of squares is 0.1618, the predicted sum of squares is 0.0403, and the total percentage predicted is 24.95%. While for the 7 landmark point analysis data was taken from 21 specimens. The value of total sum of squares is 0.1447, the predicted sum of squares is 0.0547, and the total percentage predicted is 37.85%. The regression score vs. Log centroid size (Fig. 6a) shows separate clusters for the three landmark point analysis for both the *Astriclypeus* and *Echinodiscus*, also a similar trend is observed in the Log centroid size vs. Regression score (Fig. 6b) for the seven landmark point analysis.

4. DISCUSSION

4.1 Geometric Morphometric Data Analysis

4.1.1 Three Landmark Point Data Analysis

Results showed distinctive clusters for *Astriclypeus* and *Echinodiscus*. PCA 1 and PCA 2 results constitute for a cumulative sum of 100% of the observed morphological variance present between the data sets. *Astriclypeus* samples showed more deviation in the PCA 1, while *Echinodiscus* data exhibited variation across both PCA 1 and PCA 2 axes (Fig. 4a). PCA 1 is related to the angle the lunule marked from the line of bilateral symmetry at centre of the apical disc and the line joining the outermost protruding point in curved side of the lunules towards the apical plate and the boundary respectively on the aboral surface. Morphological deformation, or morphological variation between the two genera, appears concentrated around the outermost protruding point in the curved side of the lunules towards the apical plate. This changes the angle that the lunules marked with the bilateral line of symmetry. PCA 2 appears related largely to the lunule length. These results suggested that distinct clustering of the two studied genera is mainly controlled by variation in the lunule angle and the lunule length between the two genera. Therefore, the three landmark point data analysis, which is the minimum number of landmarks needed to have a measurable area, shows that the lunules angle and length is accountable for the distinctive differentiation of the two genera.

4.1.2 Seven Landmark Point Data Analysis

Clustering trends and generic level distinctions are very much like the three-point landmark analysis. PCA 1 to 4 results contribute to a cumulative sum of approximately 95% of the observed morphological variance present between the data sets (Figs. 4b - d). The plot of PCA 1 vs. PCA 2 shows a wider distribution of *Astriclypeus* data points along the PCA 2 axis while *Echinodiscus* has a broader distribution along the PCA 1 axis; unlike the previous *Echinodiscus* results in the 3 landmark point data (Fig. 4a). Similar trends are shown in the PCA 1 vs. PCA 3 plot and PCA 1 vs. PCA 4 plot as well. PCA 1 appears to show the maximum variation the angle of the lunule makes from the line of bilateral symmetry at centre of the apical disc and the line joining the outermost point in curved side of the lunules towards the apical plate and the boundary as well as the angle variation between the left and the right lunules with respective to the plane of bilateral symmetry. Distribution of data and observed morphological variation in PCA 2 is related to the angle length (Figs. 4b - d). While observed variation between the data sets in PCA 3 and PCA 4 are related with morphological variation between the distance between the lunules as well as the angle that the lunules marked with the bilateral plan of symmetry at centre of the apical plate (Figs. 4c - d). Overall, a better visualisation of distinct clustering and differentiation of the two genera is observed in the obtained PCA results for the 7-point than the 3-point analyses.

4.2 Traditional Morphometric Data Analysis

Traditional morphometric analyses with linear measurements of the posterior lunules showed separate clusters for *Astriclypeus* and *Echinodiscus* (Figs. 5a, b).

Echinodiscus expressed a wider scatter in the data points compared to that of the genera *Astriclypeus*. This could be a result of the larger data set for *Echinodiscus* in contrast to that of *Astriclypeus*. However, the variation in the lunule length and width for the *Echinodiscus* was comparatively higher to that of the *Astriclypeus* indicating that *Echinodiscus* specimens include various stages of ontogeny and hence resulting in a wider distribution for the length and width of the lunules. Regardless, data for *Astriclypeus* and *Echinodiscus* formed two distinct clusters in our results.

4.3Analysis of Variance (ANOVA)

Regression analysis for the three landmark point data and the seven landmark point data shows distinctive clustering for both *Astriclypeus* and *Echinodiscus* (Fig. 6a). The three landmark point data shows two separate clusters with 90% confidence ellipses. However, there are some minor overlaps in the data points. This potential overlap could be due to the end members of the spectrum and this can be minimised when considering a larger data set. The seven landmark data point, also shows two separate clusters with 90% confidence ellipses with no overlap for the *Astriclypeus* and *Echinodiscus data points* (Fig. 6b).

4.4 Broader Implications

By studying *Astriclypeus mannii*, Nisiyama (1968) hypothesized a probable derivation of the genus from an ancestral genus *Amphiope* with two rounded lunules leading to the genus *Astriclypeus*. Ziegler et al. (2016) illustrated that juveniles of *A. mannii* undergoes a two key-hole stage during the early ontogeny. Seilacher (1979) outlined the clypeasteroid evolution in the paleogeographic space and hypothesized that *Astriclypeus* evolved from the two-lunule form *Amphiope* concentrated in the European strata and the Asian population of *Astriclypeus* should be derived from Indian subcontinent; thus, there should be fossil evidence recorded in the Indian subcontinent. However, there is no evidence of *Astriclypeus* reported in the fossil record for Indian subcontinent (Table 2). Instead, the closest form is *Echinodiscus* exhibiting two lunules (Srivastava 2012). Therefore, the five-lunule form *Astriclypeus* could be closely related to the two-lunule form *Amphiope* and/or *Echinodiscus*.

Based on the Cenozoic fossils recorded in the western Foothill of Taiwan, the oldest record of *Astriclypeus* fossil is from the Wuchihshan Formation (late Oligocene) of northern Taiwan, and it is abundant in the younger strata, including Talio Formation (Early Miocene), Tsoho Formation (Late Early Miocene), Nankang Formation (Middle Miocene), Toukoshan Formation (Late Pleistocene), and Holocene sediments on raised beaches (Wang 1983). Wang (1982) re-described the *Echinodiscus* from the Talio Formation of Yehliu, northern Taiwan, and currently there is no report of *Amphiope* in the Taiwan fossil records (Table 2) after decades of research. Stara and Sanciu (2014) reviewed the systematic position of astriclypeid species assigned *Amphiope* L. Agassiz, 1840 and *Echinodiscus* Leske, 1778 based on the plating pattern, morphological features such as test outline, size and shape of lunules and petals. A list of reported *Amphiope*, *Astriclypeus*, and *Echinodiscus* from India/Pakistan, Taiwan and Europe is summarized below (Table 2).

5. CONCLUSION

This study evaluates whether geometric morphometric methods can be used to differentiate between *Astriclypeus* and *Echinodiscus*, assemblages in the Yeliu Geopark based on incomplete specimens. The three landmark point analysis showed two distinctive clusters in PCA plots (Fig. 4a), which is the minimum number of landmarks that is required to have a calculable area. The differentiation is mainly based on the lunule angle from the line of bilateral symmetry at centre of the apical disc and the line joining the outermost point in curved side of the lunules towards the apical plate and the boundary respectively on the aboral surface. With the seven landmark point analysis it supported also two distinctive clusters for the two genera in the PCA plots (Figs. 4c, d). Results are supported independently based on traditional methods with linear measurements (Figs. 5a, b). Furthermore, the regression analysis also shows two separate clusters for the three landmark point and seven lanarmark point data. The major differentiation is due to the lunule angle with the plane of bilateral symmetry as well as the angles that the lunules make with each other. Hence, it is clear that the key characters for distinguishing *Astriclypeus* and *Echinodiscus* apart are the morphological differences in the lunules and lunule angles. Furthermore, geometric morphometrics can be developed into a standardized method to distinguish the generic-level and perhaps to the species-level characters for identification of key holed based on incomplete samples during broader population studies or paleoecological analyses.

Acknowledgements This work is part of Ph.D. dissertation for AS. This study was funded by the Ministry of Science and Technology, Taiwan, ROC (MOST 108-2116-M-002-014; and MOST 109-2116-M-002-020 to AS's supervisor Jih-Pai Lin; MOST 107-2811-M-002-3125; and MOST 108-2811-M-002-608 to RES).

REFERENCES

Adobe Systems Incorporated, 2002: Adobe Photoshop, Version 7.0.1, Adobe Systems Incorporated, San Jose, CA.

Bookstein, F. L., 1992: Morphometric Tools for Landmark Data: Geometry and Biology, Cambridge

Table 2. Key Oligo-Miocene species of astriclypeids reported from India/Parkistan (Srivastava 2012), Taiwan (Wang 1982, 1983, 1984, 1986), and Europe (Stara and Marini 2018).

India/Parkistan	Taiwan	Europe
Echinodiscus auritus var.	*Astriclypeus elegans*	*Amphiope bioculata*
Echinodiscus desori	*Astriclypeus mannii*	*Amphiope caronei*
Echinodiscus desori var.	*Astriclypeus miaoliensis*	*Amphiope depressa*
Echinodiscus ellipticus	*Astriclypeus pitouensis*	*Amphiope deydieri*
Echinodiscus elongatus	*Astriclypeus waiwulunensis*	*Amphiope elliptica*
Echinodiscus placenta	*Astriclypeus yeliuensis*	*Amphiope hollandei*
Echinodiscus sp.	*Echinodiscus formosus*	*Amphiope lorioli*
	Echinodiscus hsianglanensis	*Amphiope lovisatoi*
	Echinodiscus tilinensis	*Amphiope ludovici*
	Echinodiscus yeliuensis	*Amphiope montezemoloi*
		Amphiope neuparthi
		Amphiope nuragica
		Amphiope pallavicinoi
		Amphiope palpebrata
		Amphiope romani
		Amphiope sarasini
		Amphiope tipasensis
		Amphiope transversifora

University Press, Cambridge, 435 pp, doi: 10.1017/CBO9780511573064. [Link]

Bookstein, F. L., B. Grayson, C. B. Cutting, H.-C. Kim, and J. G. McCarthy, 1991: Landmarks in three dimensions: Reconstruction from cephalograms versus direct observation. *Am. J. Orthod. Dentofac. Orthop.*, **100**, 133-140, doi: 10.1016/S0889-5406(05)81520-3. [Link]

Chao, S.-M., 2000: The irregular sea urchins (Echinodermata: Echinoidea) from Taiwan, with descriptions of six new records. *Zoological Studies*, **39**, 250-265.

Dryden, I. L. and K. V. Mardia, 1998: Statistical Shape Analysis, Wiley, Chichester, 347 pp.

Hammer, Ø., D. T. A. Harper, and P. D. Ryan, 2001: PAST: Paleontological statistics software package for education and data analysis. *Palaeontologia Electronica*, **4**, 9 pp.

Hayasaka, I., 1947: Notes on some fossil echinoids of Taiwan, III. *Acta Geol. Taiwan.*, **1**, 111-128.

Kendall, D. G., 1984: Shape manifolds, procrustean metrics, and complex projective spaces. *Bull. London Math. Soc.*, **16**, 81-121, doi: 10.1112/blms/16.2.81. [Link]

Kier, P. M., 1982: Rapid evolution in echinoids. *Palaeontology*, **25**, 1-9.

Klingenberg, C. P., 2011: MorphoJ: An integrated software package for geometric morphometrics. *Mol. Ecol. Resour.*, **11**, 353-357, doi: 10.1111/j.1755-0998.2010.02924.x. [Link]

Kroh, A. and A. B. Smith, 2010: The phylogeny and classification of post-Palaeozoic echinoids. *J. Syst. Palaeontol.*, **8**, 147-212, doi: 10.1080/14772011003603556. [Link]

Mancosu, A. and J. H. Nebelsick, 2017: Ecomorphological and taphonomic gradients in clypeasteroid-dominated echinoid assemblages along a mixed siliciclastic-carbonate shelf from the early Miocene of northern Sardinia, Italy. *Acta Palaeontol. Pol.*, **62**, 627-646, doi: 10.4202/app.00357.2017. [Link]

Mihaljević, M., I. Jerjen, and A. B. Smith, 2011: The test architecture of *Clypeaster* (Echinoidea, Clypeasteroida) and its phylogenetic significance. *Zootaxa*, **2983**, 21-38, doi: 10.11646/zootaxa.2983.1.2. [Link]

Monteiro, L. R., 2013: Morphometrics and the comparative method: Studying the evolution of biological shape. *Hystrix*, **24**, 25-32, doi: 10.4404/hystrix-24.1-6282. [Link]

Mooi, R., 1989: Living and fossil genera of the Clypeasteroida (Echinoidea, Echinodermata): An illustrated key and annotated checklist. Smithsonian Contributions to Zoology, Vol. 488, Smithsonian Institution Press, 1-60, doi: 10.5479/si.00810282.488. [Link]

Nisiyama, S., 1935: On some fossil echinoids from north eastern Japan. *Saito Ho-on Kai Museum of Natural History Research Bulletin*, **5**, 131-172.

Nisiyama, S., 1968: The Echinoid fauna from Japan and adjacent regions, Part II. Palaeontological Society of Japan, Special Papers, Number 13, The Society, 491 pp.

Ohshima, H., 1927: The Illustrated Manual of the Zoology of Japan, Hokuryukan Press, Tokyo. (in Japanese)

Peng, S.-N. and S.-H. Tiao, 1971: The ecology of Taiwan sea-urchin research and study on the processing of Taiwan sea-urchin picked from its gonad (1). *Bulletin of Taiwan Fisheries Research Institute*, **18**, 129-156.

Rohlf, F. J., 2015: The tps series of software. *Hystrix*, **26**, 9-12, doi: 10.4404/hystrix-26.1-11264. [Link]

Rohlf, F. J., 2018: Tpsdig, digitize landmarks and outlines, version 2.31. Department of Ecology and Evolution, State University of New York at Stony Brook.

Rohlf, F. J. and D. Slice, 1990: Extensions of the Procrustes method for the optimal superimposition of landmarks. *Systematic Zoology*, **39**, 40-59, doi: 10.2307/2992207. [Link]

Schlüter, N., 2016: Ecophenotypic variation and developmental instability in the Late Cretaceous echinoid *Micraster brevis* (Irregularia; Spatangoida). *PLOS ONE*, **11**, e0148341, doi: 10.1371/journal.pone.0148341. [Link]

Seilacher, A., 1979: Constructional morphology of sand dollars. *Paleobiology*, **5**, 191-221, doi: 10.1017/S0094837300006527. [Link]

Shigei, M., 1981: A study on the echinoid fauna of the East China Sea and the coastal waters of southern Korea, Kyushu, Ryukyu, and Taiwan. *Publications of the Seto Marine Biological Laboratory*, **26**, 191-241.

Smith, A. B., 1984: Echinoid Palaeobiology: Special Topics in Paleontology, George Allen and Unwin, London, 190 pp.

Smith, A. B., 2001: Probing the cassiduloid origins of clypeasteroid echinoids using stratigraphically restricted parsimony analysis. *Paleobiology*, **27**, 392-404, doi: 10.1666/0094-8373(2001)027<0392:PTCOOC>2.0.CO;2. [Link]

Srivastava, D. K., 2012: An annotated bibliography of fossil echinoids (Echinodermata) of India and Pakistan. *J. Palaeontol. Soc. India*, **57**, 163-203.

Stara, P. and F. Marini, 2018: *Amphiope caronei* n. sp. (Echinoidea Astriclypeidae) from the Tortonian of Cessaniti, Vibo Valentia Province (Calabria, Italy). *Biodiversity Journal*, **9**, 73-88.

Stara, P. and L. Sanciu, 2014: Analysis of some astriclypeids (Echinoidea Clypeasteroida). *Biodiversity Journal*, **5**, 291-358.

Swisher, R. E. and J.-P. Lin, 2019: A geometric morphometric analysis of *Arachnoides placenta* (Echinoidea: Clypeasteroida): An examination of ontogenetic development and morphological variation. *Zoosymposia*, **15**, 159-171, doi: 10.11646/ZOOSYMPOSIA.15.1.18. [Link]

Wang, C.-C., 1982: On the early Miocene sand dollar Echinodiscus yeliuensis n. sp. from the Taliao Formation of Yeliu, northern Taiwan. *Proc. Geol. Soc. China*, **25**, 150-157.

Wang, C.-C., 1983: A new species of Astriclypeus from the Wuchihshan Formation near Chilung, Taiwan. *Bulletin of the Central Geological Survey*, **2**, 113-120.

Wang, C.-C., 1984: New classification of clypeasteroid echinoids. *Proc. Geol. Soc. China*, **27**, 119-152.

Wang, C.-C., 1986: Fossil astriclypeid echinoids from Taiwan. *Proc. Geol. Soc. China*, **29**, 149-183.

Webster, M. and H. D. Sheets, 2010: A practical introduction to landmark-based geometric morphometrics. *The Paleontological Society Papers*, **16**, 163-188, doi: 10.1017/S1089332600001868. [Link]

Ziegler, A., J. Lenihan, L. G. Zachos, C. Faber, and R. Mooi, 2016: Comparative morphology and phylogenetic significance of Gregory's diverticulum in sand dollars (Echinoidea: Clypeasteroida). *Org. Divers. Evol.*, **16**, 141-166, doi: 10.1007/s13127-015-0231-9. [Link]